

A comprehensive case study to the implicit and explicit approach in finite element analysis

Umit Huner¹, Gurkan Irsel^{2*} , Umut Bekar², Miroslaw Szala³ 

¹ Engineering Faculty, Mechanical Engineering Department, Kırklareli University, Kırklareli, Turkey

² Engineering Faculty, Mechanical Engineering Department, Trakya University, Edirne, Turkey

³ Faculty of Mechanical Engineering, Lublin University of Technology, Lublin, Poland

* Corresponding author's e-mail: gurkanirsel@trakya.edu.tr

ABSTRACT

The primary aim of this study is to conduct a comprehensive comparative evaluation of implicit and explicit finite element solution methodologies employed in structural analysis. This research examines the characteristics and performance differences between these two approaches, using two diverse case studies as illustrative examples. The FEM solution was performed nonlinearly by defining the linear elastic and plasticity properties of the material. The first case study focuses on a three-point bending test of a beam subjected to a slow deformation rate, while the second case study examines the damage mechanics of a pressure vessel experiencing a high deformation rate. It was found that the implicit solution method operates under the premise that displacement is independent of time, allowing for a more stable analysis in certain scenarios. On the other hand, the explicit method inherently incorporates time as a variable, making displacement a function of time. Once a solid understanding of the system's response is established, transitioning to explicit methods for more dynamic scenarios can lead to a more comprehensive and effective resolution of complex engineering problems. By carefully selecting the appropriate analysis method based on the specific characteristics of the loading conditions and the nature of the forces involved, engineers can optimize their simulations and enhance the reliability of their results.

Keywords: implicit, explicit, FEA, X section beam, pressure vessel, plasticity.

INTRODUCTION

Finite element analysis (FEA) is a powerful computational tool used to analyse and predict the behaviour of structures and materials under various conditions. Among the various methodologies employed in FEA, implicit and explicit approaches stand out as two fundamental techniques, each with its own distinct characteristics and applications. To effectively replicate an industrial process, an explicit method that is conditionally stable is best suited for scenarios where non-linearities change quickly, such as during the impact phase or stamping processes [1, 2]. Conversely, when the dynamics transition to a quasi-linear state—such as in post-impact analysis [3] or spring back simulations—an implicit method, which relies on iterative calculations, offers the benefit of unconditional stability [4, 5].

The implicit approach, often favoured for its stability and efficiency in solving static and quasi-static problems [6], utilizes a time-stepping scheme that allows for larger time increments and is particularly effective in handling complex boundary conditions and nonlinear material behaviour. In contrast, the explicit approach excels in dynamic simulations, providing a more straightforward implementation for problems involving high-speed impacts [1] and wave propagation [7], albeit at the cost of requiring smaller time steps for stability. This comparative analysis aims to explore the strengths and limitations of both implicit and explicit methods in FEA, highlighting their respective suitability for different types of engineering problems and the implications for engineers and researchers in selecting the appropriate approach for their specific applications.

Recent advancements in both explicit and implicit methods have been explored in various studies over the last decade [7–9]. For instance, research by Hai et al. [10] presents innovative strategies for enhancing the efficiency of explicit methods in large-scale simulations, while Liu et al. [6] discuss improvements in implicit algorithms that significantly reduce computational costs without sacrificing accuracy. Furthermore, combined implicit/explicit algorithms techniques into FEA has opened new avenues for optimizing both approaches, as highlighted by Noels et al. [4].

Furthermore, the choice between these methods often hinges on factors such as computational resources, desired accuracy, and the specific characteristics of the materials involved, making it essential for practitioners to thoroughly evaluate their project requirements before proceeding [7, 8]. Additionally, understanding the underlying physics of the problem can significantly influence the decision-making process, as certain scenarios may favour one method over the other based on the nature of the loading conditions and material behaviour [11, 12]. Moreover, the integration of advanced computational techniques, such as adaptive meshing [8] and parallel processing [7], can further enhance the effectiveness of these methods, allowing for more complex simulations that had better capture real-world phenomena.

Liao et al. [13] conducted a comprehensive study to investigate the dynamic structural responses and failure mechanisms of composite pressure vessels subjected to low-velocity impacts. They implemented a laminated media model using ABAQUS/Explicit, a finite element analysis software. Simulations were performed at three distinct impact energy levels to enhance understanding of the material's behaviour under varying conditions. The numerical results demonstrated good agreement with experimental data, validating the efficacy of the three-dimensional laminated media model in predicting the behaviour of composite pressure vessels under impact. Rohit et al. [14] explored the structural stability and performance of high-pressure hydrogen storage cylinders, emphasizing material selection, weight optimization, and the influence of carbon fiber on shock absorption. The performance of these cylinders was evaluated through drop and crash tests, utilizing explicit analysis within ANSYS™ Structural Analysis. While the stability of the pressure vessels was confirmed with the help of analysis, it was revealed that the drop and impact test results remained below the standards. Gavalas et al. [8]

compared the performance of implicit and explicit integration schemes for simulating the metal rolling process using commercial software packages ANSYS™ and LS-DYNA™. Their findings indicated that the explicit method generally provides higher efficiency than the implicit method, particularly as model complexity increases. Furthermore, they noted that the implicit method exhibited instabilities and numerical difficulties under certain loading conditions, adversely affecting its performance. Soares et al. [7] investigated the effectiveness of two time integration techniques: adaptive implicit–explicit (imp–exp) and explicit–explicit (exp–exp) methods. Their research provided insights into which approach yields more accurate results under specific conditions, culminating in recommendations for future studies.

Pai et al. [1] examined the crashworthiness of a buffer beam with an internal cross-section filled with various materials, employing finite element and numerical methods. Their study utilized an explicit approach in Ansys software, revealing that EPP foam-filled bumpers (C-III) demonstrated superior crashworthiness by effectively combining lightweight properties with efficient energy absorption. While some recommendations [12, 15, 16] exist regarding the use of explicit versus implicit methods based on application types, these guidelines are not exhaustive. There is a need for more detailed criteria that consider not only computational time but also factors such as material behaviour, loading conditions, and desired accuracy levels. Addressing these research gaps will enhance the understanding and application of implicit and explicit approaches in finite element analysis, leading to improved simulation outcomes across diverse engineering fields.

This study sets the stage for a deeper exploration of the explicit and implicit methodologies in finite element analysis, emphasizing their unique characteristics, applications in the field. Two case scenarios, one being a three-point bending of a beam and the other being the explosion of a pressure vessel, were examined by finite element analysis using explicit and implicit approaches by means of Ansys software. For these case scenarios, where real-time experimental data were previously obtained, the convergence of both stress and strain value to the line for implicit and explicit approaches was determined. As we delve into these methodologies, it is essential to consider the trade-offs involved in their application, particularly in terms of stability, convergence rates, and the types of problems they are best suited to solve.

METHODOLOGY

In this study, we conducted a series of case scenarios that involved two distinct types of deformation, utilizing finite element analysis (FEA) through the Ansys software. To ensure that the parameters and outcomes of the analyses were comparable, we standardized the computational resources and software settings across all simulations. Solution operations Professional 3D workstation was used for CAD and CAE operations. Properties of this workstation are A DELL PRECISION T7820 (v4) (SILVER-4114) 20 Core, 2.20 GHz, 3.00 GHz Turbo, 13.75 MB, 5GB GDDR5, 160 bit. All simulation was grounded in empirical data derived from a prior experimental setup [17], which provided critical load and boundary condition parameters essential for accurate modelling (ISO 15869 standards during structural analysis). The material was chosen as S355J0H structural steel. For the S355J0H, an elastic modulus of 210 GPa, yield strength 355 MPa, a Poisson ratio of 0.3, and a density of 7850 kg/m³ were defined for the CAD model. The strain-stress values of the material were defined in the ANSYS engineering data plasticity - multilinear isotropic hardening section obtained from experimental study [17].

Both implicit and explicit numerical methods were employed in this analysis, with each approach subjected to identical loading and boundary conditions. Two different types of loading were selected for the analysis of the X-section beam and pressure vessel.

The X-section design was created by the systematic engineering with dimensions of 150 × 100 × 5 mm (1000 mm length) in dimensions suitable for the assembly of shape-connected jaws. Irsel et al. [17] acquired the results of the

three-point bending test from a previous study. In the three point bending test, a self-wired linear strain gauge (HBM brand, 6 mm, K-factor 2.1) was affixed to a bending specimen, with stress values recorded using a 24-bit HBM-QuantumX MX840B data acquisition system. The procedure adhered to the EN ISO 7438 standard, employing a three-point bending test via an ALSA compression device at a rate of 1 mm/min. The support distance was set at 800 mm, utilizing a 6 mm HBM linear gauge (K-CLY4-0060-1-120-3-050 model) and a 22 mm HBM K-RY81-6 series rectangular rosette (0°/45°/90°). The setup included 24-bit HBM-QuantumX MX840B modules, data trace, recording computer, electronic connectors, and data cables.

The standard (EN ISO 7438) three point bending test was simulated and 100 kN force and 60 mm displacement loading were separately attempted for simulation. The results of the implicit and the explicit approaches are evaluated according to the loading type. This rigorous methodology allowed for a direct comparison of the results generated by the two techniques. For validation purposes, we utilized control data derived from previously conducted real-time experiments [17]. The empirical data collected from these experiments were instrumental in defining the load and boundary conditions applied in the simulations. Figure 1 illustrates the CAD model of beam.

In the second case study, a comprehensive analysis was conducted using a pressure vessel and a corresponding pressure test simulation. This simulation was grounded in empirical data, which provided critical load and boundary condition parameters essential for accurate modelling (ISO 15869 standards during structural analysis). The CAD model of the vessel is shown Figure 2.

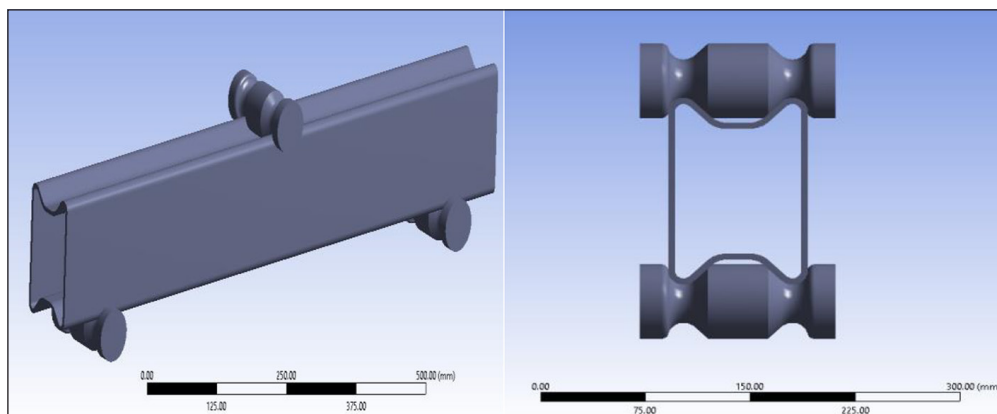


Figure 1. The CAD model of X sectioned beam

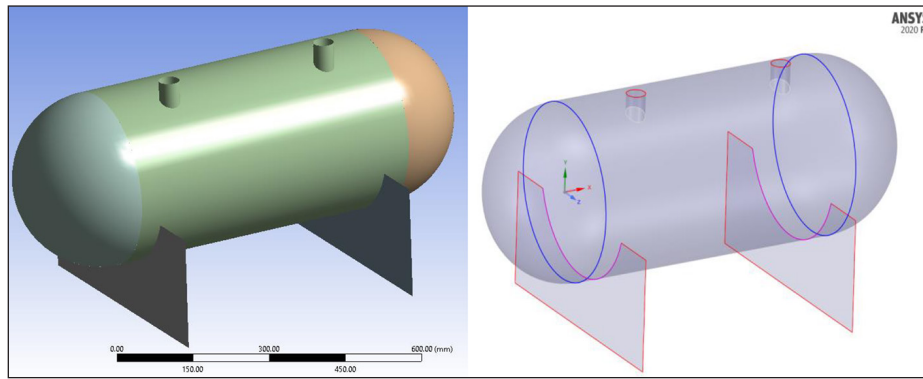


Figure 2. The CAD model (left) and design of surface model of pressure vessel (right)

Since the wall thickness is quite small compared to other dimensions, the pressure vessel was converted to a surface model with Ansys Space Claim. In addition, share topology was applied for a more suitable mesh network. Figure 2 illustrates the surface model of pressure vessel.

The pressure vessel itself was meticulously designed for this case study, constructed from a specific material known as S355J0H, which is characterized by its durability and strength under high-pressure conditions. The vessel features a wall thickness of 5 mm, ensuring structural integrity while maintaining a lightweight profile. With a cylindrical shape, the pressure vessel has a diameter of 350 mm and a length of 600 mm, dimensions that are crucial for accommodating the intended operational pressures. At either end of the cylinder, the vessel is capped with spherical ends, a design choice that enhances the overall strength and pressure distribution within the vessel. In terms of functionality, the pressure vessel is equipped with one inlet and one outlet, facilitating the controlled flow of fluids in and out of the system. This design is particularly important for applications that require precise pressure management and fluid dynamics. The entire assembly, including the vessel and its associated components, has a total weight of 49.23 kg, which is a significant factor to consider in terms of handling, installation, and operational requirements. This detailed analysis not only highlights the physical specifications of the pressure vessel but also sets the stage for understanding its performance under simulated pressure testing conditions.

FEM RESULTS

For the beam FEM study, to facilitate the analysis, a mesh size of 5 mm was implemented,

resulting in a sophisticated mesh composed of 64386 nodes and 154301, 23000 and 41220 elements for explicit and implicit solutions, respectively. The average mesh metric value was calculated to be 0.26, indicating that the mesh quality is exceptional, as referenced in established guidelines for finite element analysis. Analyses run out time were 95 min 17 sec in explicit solution and 10 min 22 sec in implicit solution for 100 kN force loading. In 60 mm displacement loading, analysis run out time was 74 min 51 sec for implicit solution and 67 min 39 sec for explicit solution.

The implicit method yielded a stress values of 355.59 MPa and 224.24 MPa end of sectional bending point for the 60 mm displacement and 100 kN force loading, respectively. When compared to the experimental data, which reported a stress value of 222.35 MPa [17], the implicit model demonstrated a deviation of only 0.08% in 100 kN loading. Figures 3 and 4 present the stress and deformations values obtained from both the 60 mm displacement and 100 kN force loading.

The solutions produced with the explicit approach are presented in Figures 5 and 6. For 60 mm deformation loading, the stress value at the middle lowest point of the beam is 329.29 MPa, whereas for 100 kN loading, the stress value at the same point is 244.22 MPa. The convergence to the experimental result is 0.09% for 100 kN loading. The implicit method generally outperforms the explicit method in terms of computational efficiency, especially as model is simple. This is attributed to the implicit method's ability to handle simple models with significantly less solution time compared to the explicit method [8].

In the implicit solution process for pressure vessel case study, a critical first step involved the careful selection of materials, where S355J0H steel was chosen for the construction of the vessel due to its favourable

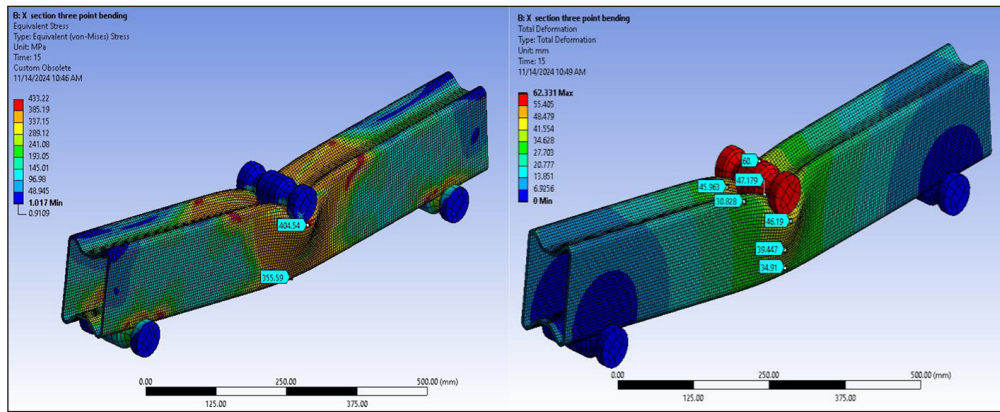


Figure 3. The finite element analysis results of the beam for 60 mm disp. loading, Equivalent stress of the beam in 60 mm disp. loading (left), The total deformation of beam (right)

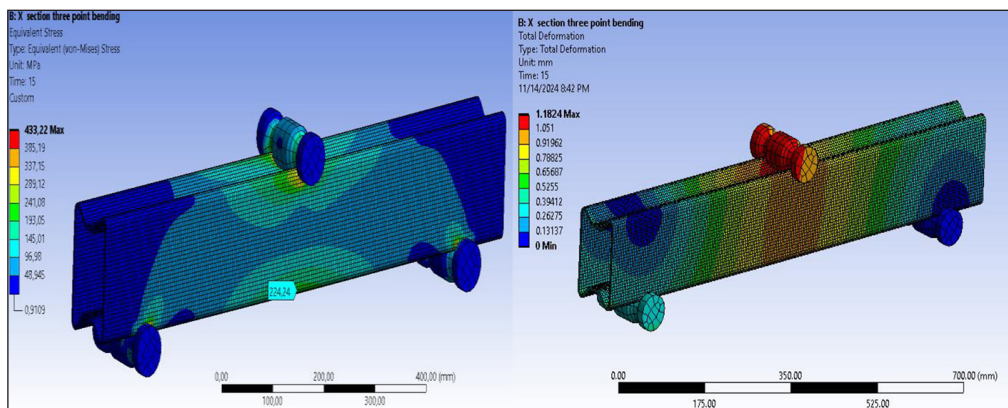


Figure 4. The finite element analysis results of beam for 100 kN force loading, The equivalent stress of beam in 100 kN force loading (left), The total deformation of beam (right)

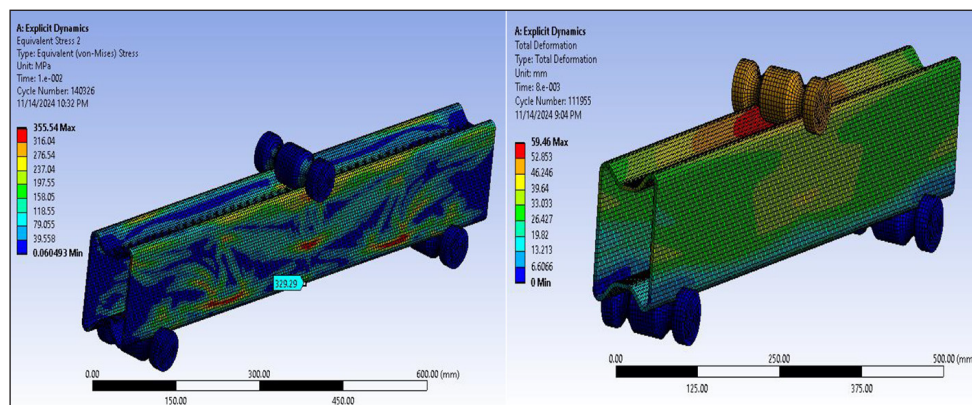


Figure 5. The explicit analysis results of the beam for 60 mm displacement loading, The equivalent stress of beam (left), the total deformation of beam (right)

mechanical properties and structural integrity. Following the material selection, the plasticity characteristics of the steel were meticulously defined to ensure accurate representation of its behaviour under stress conditions. To facilitate the analysis, a mesh size of 5 mm was implemented, resulting in a sophisticated

mesh composed of 48,820 nodes and 48,693 elements. The average mesh metric value was calculated to be 0.05. It was determined that the pressure vessel designed with the empirical formulation would catastrophically deform at a pressure of 18 MPa for the S355J0H steel (yield strength 355 MPa). Therefore,

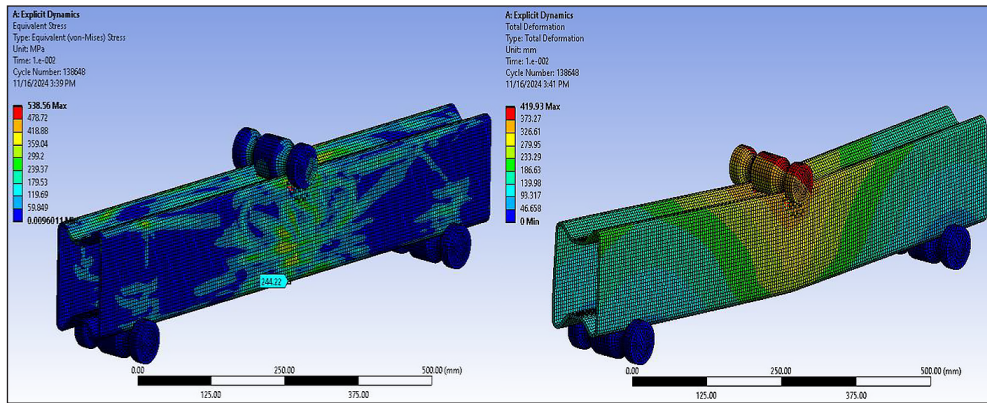


Figure 6. The explicit analysis for 100 kN force loading, equivalent stress (left), total deformation (right)

in order to further investigate the explicit and implicit approach, analyses were performed for a loading of 5 MPa where the pressure vessel was not damaged and a loading of 18 MPa where the pressure vessel was suddenly damaged. The empirical results for pressure vessel exhibits 175 MPa stress in shell and 87.5 MPa in head for 5 MPa pressure loading. For the 18 MPa pressure loading, empirical solution exhibit stress values of 630 MPa in shell and 315 MPa in the head of pressure vessel. For the 5 MPa loading, the

analysis results obtained with the implicit approach are shown in Figure 7. Analyses run out time were 17.8 sec for the implicit solution, 32 min 13 sec for the explicit solution. A stress of 178.35 MPa was observed in the region where the deformation due to the pressure was the maximum possible. It was also observed that the displacement for the same region was around 0.2967 mm. When the solutions for 18 MPa are analysed (Fig. 8), we encounter a stress of 525.69 MPa and a deformation of 549.95 mm. Even, it was

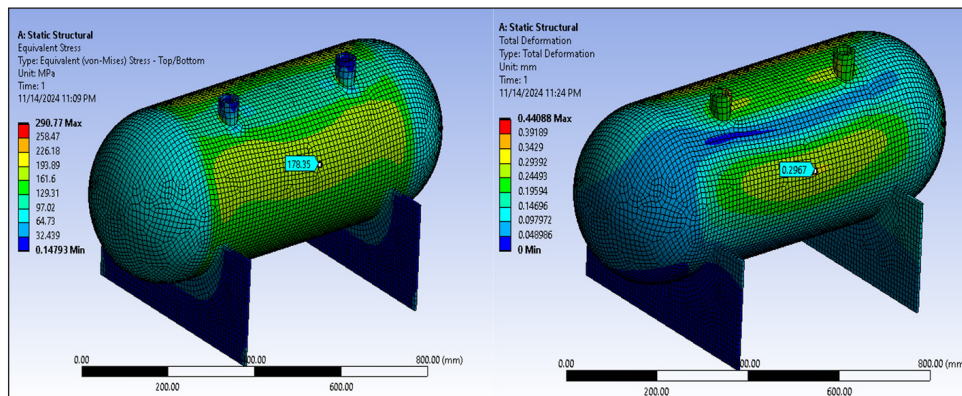


Figure 7. The implicit analysis results for 5 MPa pressure loading, The equivalent stress (left), The total deformation (right)

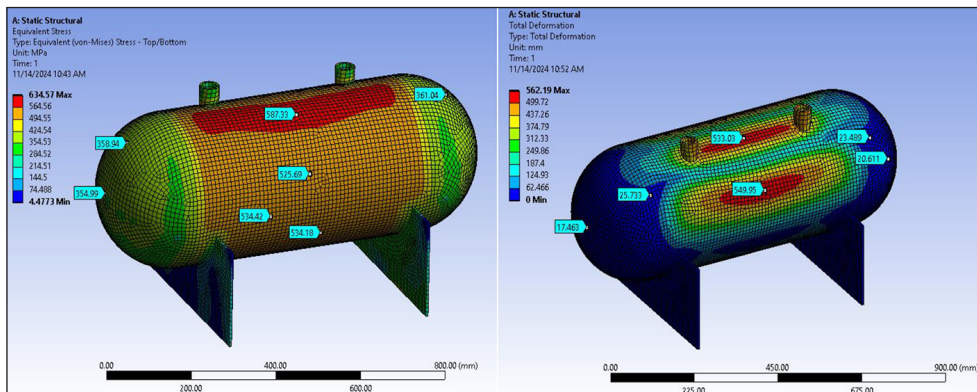


Figure 8. The implicit analysis results for 18 MPa pressure loading, equivalent stress (left), Total deformation (right)

determined that although the deformation was very large, it was not shown in real scale. This will be discussed in the discussion section.

In addition to the meticulous mesh design, it is crucial to consider the impact of frictional interactions on the overall analysis. The selection of appropriate contact conditions significantly influences stress distribution and deformation patterns within the vessel structure. For instance, a friction coefficient set at 0.2 between the steel surfaces can lead to variations in force transmission that may not be captured adequately with a simplistic model [3, 18]. Furthermore, incorporating advanced material models that account for strain rate sensitivity could enhance the accuracy of predictions under dynamic loading scenarios, as evidenced by studies comparing different finite element methods [13, 19, 20]. This holistic approach to modeling ensures that both mechanical properties and operational conditions are accurately represented, ultimately leading to more reliable structural assessments.

Figure 9 shows the explicit analysis results for deformation and equivalent stress in 5 MPa

pressure loading. The elapsed run time was 2 min 8 sec. This specific pressure level was previously identified in an empirical calculation as the threshold at which the vessel do not damage, highlighting its critical importance in assessing the vessel’s integrity. From the simulation results, the maximum stress value recorded was approximately 200.62 MPa, which aligns closely with the empirical calculation of 210 MPa.

The 18 MPa pressure was applied to the pressure vessel and the results of the explicit analysis are shown in Figure 10. The elapsed run time in solver was 281.627 min. The visuals of the analysis result show that catastrophic damage occurred in the pressure vessel. Considering that the empirically obtained results of the pressure vessel are also considered as the damage limit, it can be said that the visual results are consistent. In the area of the pressure vessel where the damage occurred, a stress of approximately 600.95 MPa occurred, while the deformation showed a very large value of 1.001e5 mm.

Overall, these findings illustrate that in structural analyses involving large deformations, the

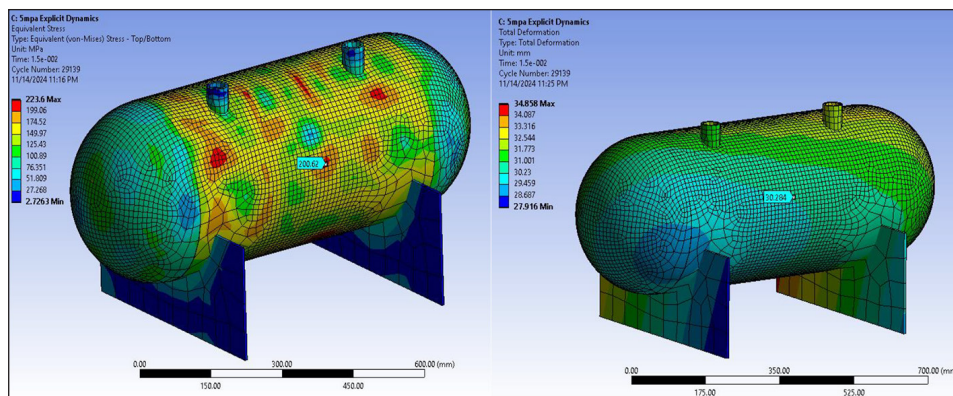


Figure 9. Implicit analysis results of pressure vessel in 5 MPa loading, equivalent stress (left) and total deformations (right)

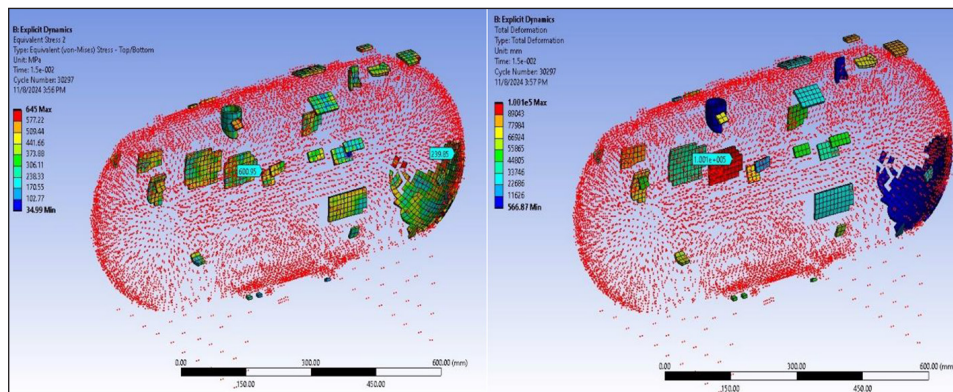


Figure 10. The deformations and equivalent results of pressure vessel for the 18 MPa pressure loading.

explicit approach not only provides a robust framework for understanding material behaviour under extreme conditions but also yields results that are closely aligned with empirical observations, thereby enhancing confidence in its application for future studies and design considerations in pressure vessel engineering.

DISCUSION

In this study, two distinct scenarios were meticulously examined to analyse the behaviour of structural elements under various loading conditions. The first scenario involved a beam characterized by an X-shaped cross-section, which was subjected to bending forces. Specifically, the analysis focused on a three-point bending test model where the beam experienced a substantial load of 100 kN alongside a notable displacement of -60 mm. The results of this investigation revealed critical insights into the material behaviour under stress. As depicted in Figure 11, the implicit solution derived from the analysis indicated that the 60 mm deformation

of the X-shaped cross-section beam surpassed the yield strength threshold of the S355J0H material, which is established at 355 MPa. This outcome led to the onset of plastic deformation, highlighting the importance of understanding plasticity in the context of structural integrity. The definition of plasticity was integral to the solution process, facilitating a damage simulation that closely mirrored real-world conditions and behaviours. A noteworthy observation arose when comparing the two simulations. As illustrated in Figure 12, despite employing identical solution definitions and mesh sizes, the outcomes diverged significantly. The implicit analysis method necessitated iterative processes to achieve solution convergence, which is a critical aspect of ensuring accuracy in complex simulations. In contrast, the explicit analysis method did not require such iterations, leading to a more straightforward computational approach. For the beam experiencing a 60 mm deflection, the simulation was conducted within a remarkably brief solution time of 0.01 seconds. While this rapid computation yielded stress values that were relatively realistic, it also resulted in a damage pattern

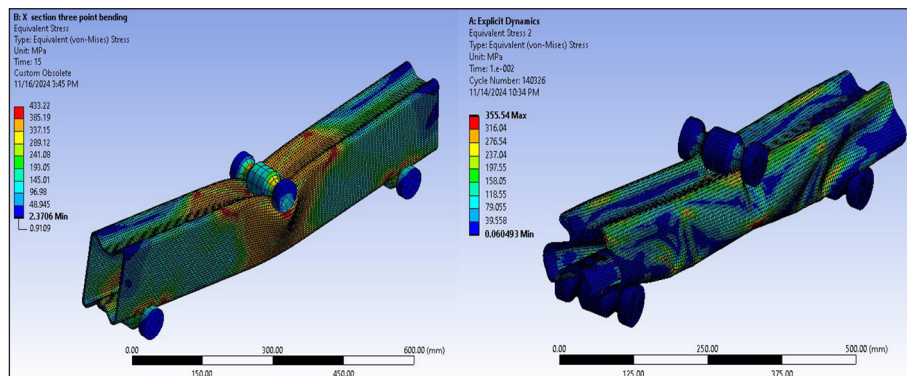


Figure 11 The true scale equivalent stress for 60 mm disp. loading, the implicit solution (left), the explicit solution (right)

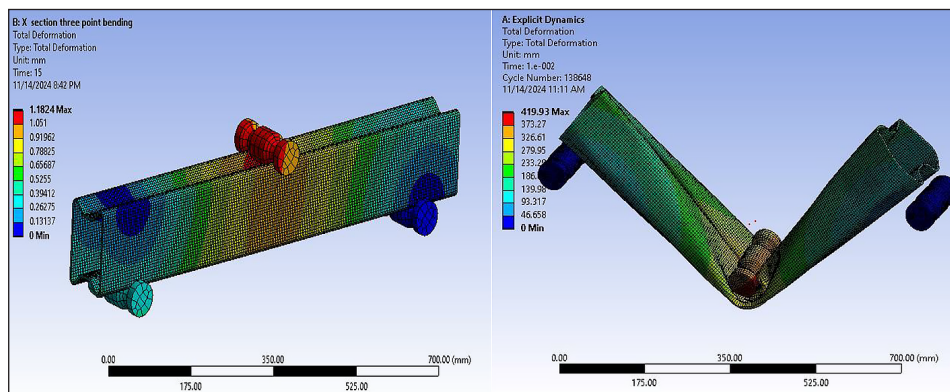


Figure 12. The explicit analysis results on true scale for 100 kN force loading, the implicit total deformation (left), the explicit total deformation (right)

simulation that lacked the precision observed in the implicit analysis. This discrepancy underscores the inherent trade-offs between speed and accuracy in computational simulations, emphasizing the need for careful consideration of the chosen analysis method based on the specific requirements of the engineering problem at hand.

When a load of 100 kN is applied to the beam, the implicit solution reveals damage patterns that correspond closely with the static loading configuration that was previously assessed (refer to Figure 13 for visual reference). This alignment suggests that the implicit analysis effectively captures the expected stress distribution and resultant damage under static conditions. In contrast, Figure 13 illustrates the damage simulation derived from the implicit analysis, which appears to provide a more accurate representation of real-world conditions.

This discrepancy highlights the advantages of explicit methods in capturing the dynamic response of materials under load, reflecting the complexities of actual behaviour more faithfully than the implicit approach. However, it is important to note that the analysis has its limitations, particularly concerning the geometric irregularities present at the ends of the beam. These irregularities do not accurately reflect the physical reality of the beam’s structure, indicating a potential area for refinement in the modelling process. Such discrepancies could lead to misinterpretations of the beam’s performance under load, underscoring the need for careful consideration of geometric factors in future analyses.

Since the loading pattern of the pressure vessel occurs in a short time (6 seconds, in damage moment 0.02 sec) compared to the beam loading pattern, this loading pattern is considered as a dynamic process (Fig. 14). As a result of the solution methods evaluated for simulating the damage of this vessel, it

is observed that the actual damage pattern is consistent with the explicit solution method.

The correlation between simulated and empirical data underscores the reliability of the explicit approach in predicting stress responses under high-pressure conditions. Furthermore, the simulation indicated that the deformation of the container at the moment of failure reached around $1.001e5$ mm. Such proximity in values reinforces the validity of the simulation results, particularly in scenarios characterized by significant deformations. In some studies [1, 21, 22], the explicit approach was used in extreme conditions such as drops and crashes, and its convergence and reliability to real experimental results were tested by simulation.

In addressing complex engineering problems, two primary methodologies can be employed to derive solutions, both of which ultimately yield comparable stress values. However, when it comes to simulating damage, the explicit simulation method tends to provide a more accurate representation of real-world phenomena, particularly during scenarios involving shock impacts and dynamic loading conditions [1, 5, 22]. On the other hand, the implicit method excels in delivering realistic outcomes in static loading situations, where forces are applied gradually and remain constant over time. From an efficiency standpoint, explicit solutions are significantly advantageous, requiring approximately 45% less computational time to implement compared to their implicit counterparts. Implicit methods often demand greater processing power and longer durations for convergence, as they involve solving a series of equations iteratively to ensure accuracy at each step. This makes the explicit approach an attractive option for engineers seeking to streamline their analyses without compromising on accuracy. In practice, a prudent engineering strategy would begin with the implicit method for a preliminary

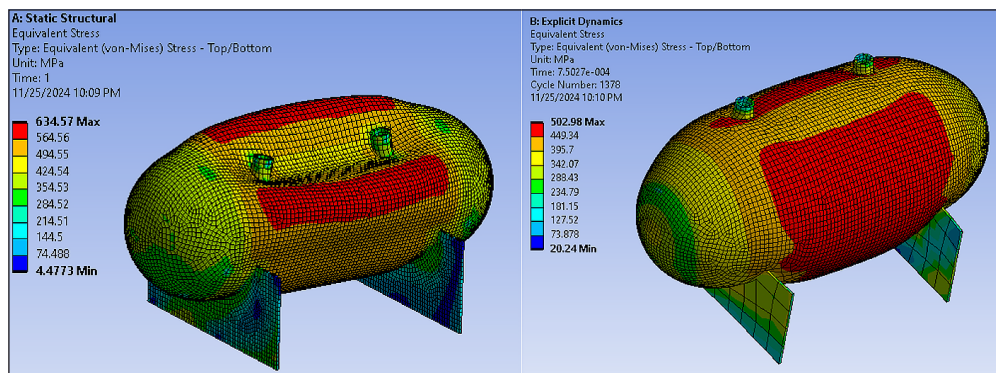


Figure 13. The implicit (true scale) total deformation result (left) and the explicit stress results of pressure vessel (right)

evaluation of the system's overall load-bearing capacity. This initial assessment can help identify potential weaknesses before transitioning to explicit solutions for a more detailed analysis of dynamic events. Moreover, the size of elements used in explicit simulations plays a critical role in influencing the overall solution time. Smaller elements can lead to more accurate representations of the physical behaviour but can also increase computational demands. In contrast, implicit solutions are more sensitive to element errors, as convergence is required for each step in the analysis. If errors occur in the elements, they cannot be corrected, potentially resulting in inaccurately high-stress predictions. Explicit analysis, conversely, is generally more resilient to element inaccuracies, making it a more robust choice in many scenarios [4, 7].

As a rule of thumb, if the event being analysed is dynamic and occurs over a short time frame, explicit analysis is the preferred method. Conversely, for static systems where loads remain unchanged over time, the implicit method is typically recommended for its accuracy and reliability. This nuanced understanding of both methodologies allows engineers to select the most appropriate approach based on the specific characteristics of the problem at hand.

CONCLUSIONS

This study presents a thorough comparison of stress and deformation values obtained through implicit and explicit computational methods, revealing critical insights into their respective efficiencies and accuracy.

The selection of the analysis method is the first step in obtaining results that align with reality. To choose an appropriate method for the problem, case studies were solved on computer with the same mesh size and processor. The effects of applying different methods to the same problem were clearly demonstrated based on the empirical and experimental studies conducted. General recommendations for engineering solutions were provided. The overall conclusion drawn is that if the event being analyzed is a dynamic case occurring within seconds, the explicit analysis method should be preferred; whereas, for static systems where the load does not change over time, the implicit method should be used. Additionally, all material-specific properties relevant to the materials used must be defined accurately to ensure a correct

solution. More specific results obtained from the comparative analysis of cases are as follows:

For the beam simulation, the implicit method demonstrated a commendable performance, yielding a stress value of 224 MPa with a deviation of only 1% from experimental data, while the explicit method provided a higher stress value of 244 MPa, showing a larger discrepancy of 9.23%. In this case, where no major deformation occurred, there was no significant difference between the stress values, while considering the solution times, an implicit solution time of 10 min 22 seconds and an explicit solution time of approximately 95 minutes were obtained. In addition, the deformation results and visualizations were more realistic in the implicit solution. In the scenario of high pressure loading of the pressure vessel, implicit showed a stress result of 525 MPa, while explicit showed a stress result of 600 MPa. Both values theoretically indicate that catastrophe damage will occur. Deformation values and images revealed a result close to reality in the explicit solution. This correlation not only enhances our understanding of vessel integrity under extreme conditions but also establishes a strong foundation for future research and design practices in pressure vessel engineering, ensuring that safety and performance standards are met in real-world applications.

Ultimately, this study contributes to the ongoing discourse on computational methods in material analysis, emphasizing the importance of method selection to optimize accuracy and efficiency in engineering applications.

Acknowledgements

The author(s) disclosed receipt of the following financial support for the research, authorship, and/or publication of this article: This work was supported by the Trakya University Scientific Research Projects Coordination Unit (TURKEY) by TUBAP 2022/102

REFERENCES

1. Pai A., Kalliyath S.A, Rodriguez-millan M, Shenoy B. Crashworthiness analysis of filled / unfilled automotive bumper beams subjected to head-on collision events: a numerical approach. *Cogent Eng* 2024; 11. <https://doi.org/10.1080/23311916.2024.2399737>.
2. Cai W., Wen Z., Jin X., Zhai W. Dynamic stress analysis of rail joint with height difference defect using finite element method 2007; 14: 1488–1499.

- <https://doi.org/10.1016/j.engfailanal.2007.01.007>.
3. Ringsberg J.W., Li Z., Johnson E., Kuznecovs A. Reduction in ultimate strength capacity of corroded ships involved in collision accidents accidents 2018; 5302. <https://doi.org/10.1080/17445302.2018.1429158>.
 4. Noels L., Stainier L., Ponthot J.P. Combined implicit/explicit algorithms for crashworthiness analysis. *Int J Impact Eng* 2004; 30: 1161–1177. <https://doi.org/10.1016/j.ijimpeng.2004.03.004>.
 5. Bau I., Umwelt G., Leidinger L.F. Explicit isogeometric b-rep analysis for nonlinear dynamic crash simulations integrating design and analysis by means of trimmed multi-patch shell structures 2020.
 6. Liu J.L., Qin L.Y., Wu S.Y., Yan J.Y. An efficient iterative method for vehicle - track nonlinear coupled dynamic analysis based on explicit and implicit algorithms 2024. <https://doi.org/10.1007/s42417-024-01504-y>.
 7. Soares D., Sales I de S., Pinto L.R., Mansur W.J. A study on adaptive implicit–explicit and explicit–explicit time integration procedures for wave propagation analyses. *Acoustics* 2024; 6: 651–680. <https://doi.org/10.3390/acoustics6030036>.
 8. Gavalas E. Mesh sensitivity analysis on implicit and explicit method for rolling simulation 2018; 9: 465–474. <https://doi.org/10.1108/IJSI-07-2017-0046>.
 9. Kut S., Stachowicz F. Bending moment and cross-section deformation of a box profile. *Adv Sci Technol Res J* 2020; 14: 85–93. <https://doi.org/10.12913/22998624/118552>.
 10. Hai L., Zhang H., Wriggers P., Huang Y jie., Feng Y., Junker P. A novel semi-explicit numerical algorithm for efficient 3D phase field modelling of quasi-brittle fracture. *Comput Methods Appl Mech Eng* 2024; 432: 117416. <https://doi.org/10.1016/j.cma.2024.117416>.
 11. Paper O. Computationally efficient stress reconstruction from full-field strain 2024; 0: 849–872. <https://doi.org/10.1007/s00466-024-02458-4>.
 12. Song H., Yang J., Du X., Wang M. Explicit-explicit sequence calculation method for the wheel / rail roll- ing contact problem based on ANSYS/LS-DYNA 2015; 3.
 13. Liao B.B., Jia L.Y. Finite element analysis of dynamic responses of composite pressure vessels under low velocity impact by using a three-dimensional laminated media model. *Thin-Walled Struct* 2018; 129: 488–501. <https://doi.org/10.1016/j.tws.2018.04.023>.
 14. Rohit G., Santosh M.S., Kumar M.N., Raghavendra K. Numerical investigation on structural stability and explicit performance of high-pressure hydrogen storage cylinders. *Int J Hydrogen Energy* 2023; 48: 5565–5575. <https://doi.org/10.1016/j.ijhydene.2022.11.154>.
 15. Liu P.F., Xing L.J., Zheng J.Y. Failure analysis of carbon fiber/epoxy composite cylindrical laminates using explicit finite element method. *Compos Part B Eng* 2014; 56: 54–61. <https://doi.org/10.1016/j.compositesb.2013.08.017>.
 16. Miłek T. Experimental determination of material boundary conditions for computer simulation of sheet metal deep drawing processes. *Adv Sci Technol Res J* 2023; 17: 360–373. <https://doi.org/10.12913/22998624/172364>.
 17. İrsel G. Experimental, analytical, and numerical investigations on the flexural and fatigue behavior of steel thin-walled X-section beam. *Proc Inst Mech Eng Part C J Mech Eng Sci* 2022; 236: 11041–11065. <https://doi.org/10.1177/09544062221111053>.
 18. He L., Jiang Y., Zhang W. Effect of jack thrust angle change on mechanical characteristics of shield tunnel segmental linings considering additional constrained boundaries. *Appl Sci* 2022; 12. <https://doi.org/10.3390/app12104855>.
 19. Tran H.T. A new energy-based local damage model for dynamic analysis of. *Comput Mech* 2024. <https://doi.org/10.1007/s00466-024-02547-4>.
 20. Tian K., Zhi J., Tan V.B.C, Tay T.E. An explicit finite element discrete crack analysis of open hole tension failure in composites. *Compos Struct* 2024; 345: 118411. <https://doi.org/10.1016/j.compstruct.2024.118411>.
 21. Skrzat A., Wójcik M. Numerical modeling of superplastic punchless deep drawing process of a TI-6AL-4V titanium alloy. *Adv Sci Technol Res J* 2020; 14: 127–136. <https://doi.org/10.12913/22998624/114029>.
 22. Nieoczym A., Drozd K. Fractographic assessment and FEM energy analysis of the penetrability of a 6061-T aluminum ballistic panel by a fragment simulating projectile. *Adv Sci Technol Res J* 2021; 15: 50–57. <https://doi.org/10.12913/22998624/129951>.